Communication

Morphogenesis of Highly Ordered Mixed-Valent Mesoporous Molybdenum Oxides

Jinglu Chen, Christian Burger, Chirakkal V. Krishnan, and Benjamin Chu

J. Am. Chem. Soc., **2005**, 127 (41), 14140-14141• DOI: 10.1021/ja054023v • Publication Date (Web): 23 September 2005

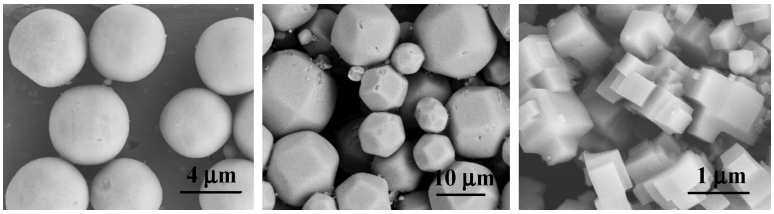

More About This Article

J|A|C|S
COMMUNICATIONS

Published on Web 09/23/2005

Morphogenesis of Highly Ordered Mixed-Valent Mesoporous Molybdenum Oxides

Jinglu Chen, Christian Burger, Chirakkal V. Krishnan, and Benjamin Chu*

Chemistry Department, Stony Brook University, Stony Brook, New York 11794-3400

Received July 1, 2005; E-mail: bchu@notes.cc.sunysb.edu

Following the discovery of ordered mesoporous molecular sieves MCM-41,[1] zeolites and other silicate/aluminosilicate mesoporous materials attracted considerable attention.[2] Thereafter, many other non-silica oxide mesoporous materials have been reported.[3] Mesostructures with mixed oxidation states may be synthesized for metals with partially filled d-shells, which can be used as versatile systems for redox catalysis and battery applications. Mixed oxidation state mesoporous manganese oxides have recently been synthesized by means of the oxidation of Mn(OH) in a template of aqueous cetyltrimethylammonium bromide cationic surfactant micelles.[4] Toroidal mesoporous molybdenum oxide with mixed V and VI oxidation states was also prepared by aging the as-synthesized dimeric molybdenum ethoxide complex with a bridging dodecylimido group as the structure-constructing block at 90 °C.[5]

The macroscopic morphology of mesostructured materials was an important feature in considering their practical applications, such as in optoelectronic devices. Many efforts have been made to control the morphology of mesoporous silica-based materials.[6] However, very little study has been focused on the morphological control of mesoporous transition metal oxides, which are expected to have unique optoelectronic and photocatalytic properties over silica materials.[7] Here we report a convenient procedure for the morphogenesis of highly ordered mixed-valent molybdenum oxide mesostructures with well-defined shapes, *without* involving the use of amphiphilic surfactants *or* the preparation of metal alkyloxide precursors.

The yellow peroxomolybdenum precursor solution (1.0 M) was prepared by dissolving molybdenum metal powder in 30% H_2O_2.[8] Poly(ethylene oxide) (PEO) homopolymer, instead of amphiphilic block copolymer surfactants, was selected as a structure-directing agent and a reducing agent. A yellow molybdenum precursor solution and a PEO solution were mixed at a molar ratio of [Mo]:[EO] (ethylene oxide repeating unit) = 1:5. The mixed solution was then exposed to ultrasound irradiation for 12 h without cooling so that a temperature of about 70 °C was reached at the end of the reaction. After sonication, the reaction solution became dark blue, and finally blue precipitates appeared in the bottom of the reaction vial. The precipitates were washed several times with large amounts of water, centrifuged, and dried under vacuum at room temperature.

An X-ray diffraction (XRD) pattern of the as-prepared molybdenum blue precipitates from PEO with a molar mass of 1×10^5 g/mol (PEO-100K) is shown in Figure 1a. Unlike the XRD patterns reported previously for other mesoporous materials, in which only a few reflection peaks were detected, the pattern in Figure 1a showed more than 60 well-resolved reflections, covering a wide s range from 0.19 to 2.4 nm^{-1} (scattering vector $s = 2 \sin \theta/\lambda$, with 2θ being the scattering angle). All these reflections can be indexed on a primitive cubic cell with lattice constant $a = 5.1$ nm. The large number of well-resolved reflections allows them to be distinguished unambiguously between body-centered and primitive cubic due to the absence of the $7^{1/2}$, $15^{1/2}$, $23^{1/2}$, ... reflections. The appearance of very high order reflections and the first-order d

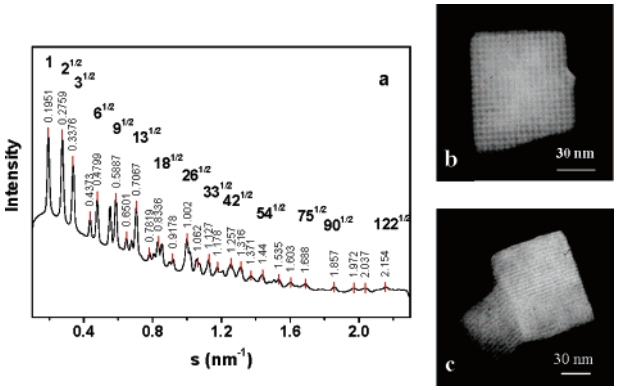

Figure 1. (a) XRD pattern of as-prepared blue molybdenum oxide from PEO-100K. TEM images of extracted molybdenum oxide from PEO-100K recorded along the [100] (b) and [110] (c) zone axes.

spacing of 5.1 nm indicated that the obtained blue product was an extremely ordered mesostructured material. We have previously observed materials with similar XRD patterns in a synthesis not involving sonication after very long reaction times.[9] Figure 1b,c shows transmission electron microscopy (TEM) images of mesostructured molybdenum oxide from PEO-100K recorded along the [100] and [110] zone axes of the mesostructure, respectively. Parallel-aligned mesoscale channels with a spacing of about 5 nm were clearly observed. The channels were to arrange in a square lattice, with mesopore and wall diameters both being about 2.5 nm. This TEM finding is fully consistent with the XRD result.

Scanning electron microscopy (SEM) images of precipitated molybdenum oxide samples from PEO solution with different PEO molar masses are shown in Figure 2. We can see that the final product is composed of very uniform particles both in size and in shape, which are closely related to the molecular chain length of the polymer used during preparation. With a short-chain polymer additive, loosely assembled polyhedral particles with an average size of 2 μm were obtained (Figure 2a, PEO-400), partially due to the poor structure-directing ability of short-chain molecules. Upon increase of the molar mass of PEO to 4.6×10^3 g/mol, ball-like structures were obtained with an average diameter of 3 μm (Figure 2b, PEO-4600). After the molar mass of PEO was further increased to 1×10^4 g/mol, both ball-like morphology (average diameter of 3 μm) and well-shaped polyhedral morphology (average size of 600 nm) coexisted in the final product (Figure 2c, PEO-10K), due presumably to partial degradation of PEO chains upon sonication. The polyhedral particle is a rhombic dodecahedron with 12 well-defined crystal faces (also see Figure S1 in the Supporting Information), which can be described as a truncated cube. When the molar mass of the applied PEO reached 1×10^5 g/mol, uniform cubic particles (~400 nm) with sharp edges and corners were obtained exclusively (Figure 2d). Upon further increases in the molar mass of PEO to 6×10^5, 1×10^6, or 5×10^6 g/mol, only

10.1021/ja054023v CCC: $30.25

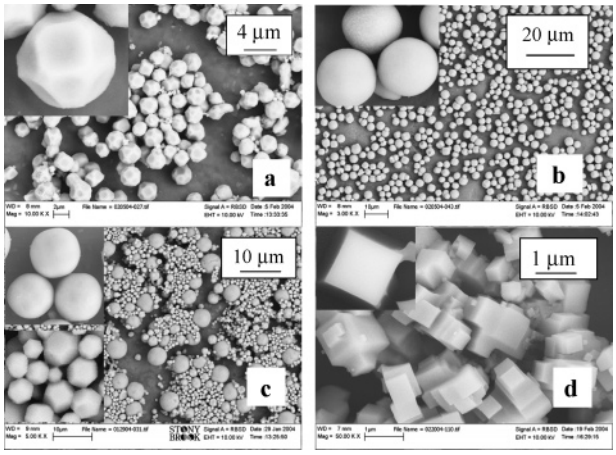

Figure 2. SEM images of mesostructured molybdenum oxides prepared from PEO with different molar masses: (a) PEG-400, (b) PEG-4600, (c) PEG-10K, (d) PEO-100K ([Mo]:[EO] = 1:5). The insets show high magnification images.

cubic morphologies with a uniform size of ~400 nm were obtained. It should be noted that all these samples prepared from PEO with different molar masses showed exactly identical XRD patterns, indicating the existence of the same basic structure unit despite their differences in the assembled morphology of the final products. While the presence of polyol additives (small molecules like ethylene glycol and glycerol) did not yield any structured materials, the color of the reaction solution changed to dark blue after sonication, indicating the essential role of long polymer chains in the formation of assembled morphology.

The presence of the PEO homopolymer plays two roles in the formation of mesostructured materials: (1) it acts as a weak reducing agent to partially reduce Mo(VI) to Mo(V) or Mo(IV); (2) the chain length of PEO controls the morphology of the final product by possibly forming crown ether-like PEO−Mo complexes. The reduction of Mo(VI) was observed as the color change of the reaction solution from yellow to dark blue during sonication. If no PEO was added, the final product was yellow molybdenum oxide monohydrate ($MoO_3 \cdot H_2O$) crystals.

The reducing ability of PEO has been reported in the formation of gold and silver particles.[10] Multivalent metal species could be bound to the pseudo-crown ether cavities (formed by coiled PEO molecules) through weak coordination bonds and then reduced. In this case, the Mo(VI) precursor was bound to the oxyethylene groups of a long PEO chain through coordination interaction. The resulting Mo−PEO complex was then reduced and assembled into specific shapes during ultrasonic irradiation. As to the morphological control of the final product over the molar mass of PEO as shown in Figure 2, one possibility could be the viscosity effect of the reaction solution due to the different molar masses of polymer, or the molecular chain length of PEO could determine the overall shape of Mo−PEO complex that controlled the morphology of the final product. To prove this point, we carried out another set of experiments, increasing the concentration of low molar mass PEO ([Mo]:[EO] = 1:20), decreasing the concentration of high molar mass PEO ([Mo]:[EO] = 2:5), or mixing both low and high molar mass PEO at 1:1 by weight (total [Mo]:[EO] = 1:10). The SEM results show that increasing the concentration of low molar mass PEO did not lead to the formation of cubic morphology, and decreasing the concentration of high molar mass PEO could not lead to the formation of ball-like or polyhedral morphologies (Figure S1). The presence of both low and high molar mass PEO in the reaction solution leads to the formation of mixed ball-like and cubic particles in the final product. These results indicated that the viscosity of the reaction solution was not a factor controlling the morphology of the final product. However, the molecular chain length played a key role in determining the assembled morphology of the product through the formation of PEO−Mo complex with slightly different network structures according to the molecular chain length of PEO. On the other hand, decreasing the concentration of PEO results in the formation of fibrous molybdenum trioxide monohydrate crystals besides the mesostructured molybdenum oxide cubes or polyhedrons (Figures S2b and S2c, Supporting Information), due to the insufficient amount of PEO as the reducing agent.

Thermogravimetric analysis (TGA) was used to determine the average oxidation state of the molybdenum atom by comparing the weight loss difference of the TGA curves recorded in N_2 atmosphere (final form: MoO_x) and air atmosphere (final form: MoO_3), respectively. The relative weight loss difference in air and in nitrogen (4.7%) corresponded to the relative weight gain of the transformation from MoO_x to MoO_3, from which we obtained a value of 2.4 for x. This mixed-valent oxidation state of IV, V, and VI corresponds to an average oxidation state of 4.8 for molybdenum in the mesostructure, and is fully consistent with the result obtained from cerimetric titration.

A nitrogen adsorption−desorption isotherm was measured to check whether the mesopores were open and accessible. A diagnostic type IV isotherm with very little hysteresis was observed (Figure S2).[11] The Brunauer−Emmett−Teller (BET) surface area was found to be 212 m^2/g, which is the highest surface area observed for synthesized molybdenum oxide materials. The average mesopore diameter was about 2.4 nm, calculated by the Barrett−Joynes−Halenda (BJH) method, very close to that seen in TEM images. The small amount of hysteresis suggested that the pores were very uniform and there was very little obstruction of the channels in the mesoporous morphology, allowing for the almost reversible adsorption and desorption of nitrogen to take place.

Acknowledgment. B.C. acknowledges the support of this work by the U.S. Department of Energy (DEFG0286ER45237.023) and of the X27C beamline (DEFG0299ER45760) at NSLS, BNL. The authors are indebted to Prof. Clare P. Grey for BET measurements.

Supporting Information Available: Experimental procedures, SEM images, Raman spectra, and nitrogen adsorption−desorption isotherm of extracted mesoporous materials. This material is available free of charge via the Internet at http://pubs.acs.org.

References

(1) Kresge, C. T.; Leonowicz, M. E.; Roth, W. J.; Vartuli, J. C.; Beck, J. S. *Nature* **1992**, *359*, 710.
(2) (a) Attard, G. S.; Glyde, J. C.; Goltner, C. G. *Nature* **1995**, *378*, 366. (b) Bagshaw, S. A.; Prouzet, E.; Pinnavaia, T. J. *Science* **1995**, *269*, 1242. (c) Zhao, D. Y.; Feng, J. L.; Huo, Q. S.; Melosh, N.; Fredrickson, G. H.; Chmelka, B. F.; Stucky, G. D. *Science* **1998**, *279*, 548. (d) Landskron, K.; Ozin, G. A. *Science* **2004**, *306*, 1529.
(3) (a) Yang, P. D.; Zhao, D. Y.; Margolese, D. I.; Chmelka, B. F.; Stucky, G. D. *Nature* **1998**, *396*, 152. (b) Attard, G. S.; Bartlett, P. N.; Coleman, N. R. B.; Elliott, J. M.; Owen, J. R.; Wang, J. H. *Science* **1997**, *278*, 838. (c) Kim, T. W.; Park, I. S.; Ryoo, R. *Angew. Chem., Int. Ed.* **2003**, *42*, 4375.
(4) Tian, Z. R.; Tong, W.; Wang, J. Y.; Duan, N. G.; Krishnan, V. V.; Suib, S. L. *Science* **1997**, *276*, 926.
(5) Antonelli, D. M.; Trudeau, M. *Angew. Chem., Int. Ed.* **1999**, *38*, 1471.
(6) (a) Grun, M.; Lauer I.; Unger, K. K. *Adv. Mater.* **1997**, *9*, 254. (b) Yang, H.; Coombs, N.; Ozin, G. A. *Nature* **1997**, *386*, 692. (c) Yu, C.; Tian, B.; Fan, J.; Stucky, G. D.; Zhao, D. *J. Am. Chem. Soc.* **2002**, *124*, 4556.
(7) Dong, A.; Ren, N.; Tang, Y.; Wang, Y.; Zhang, Y.; Hua, W.; Gao, Z. *J. Am. Chem. Soc.* **2003**, *125*, 4976.
(8) Dickman, M. H.; Pope, M. T. *Chem. Rev.* **1994**, *94*, 569.
(9) Liu, T.; Wan, Q.; Xie, Y.; Burger, C.; Liu, L.; Chu, B. *J. Am. Chem. Soc.* **2001**, *123*, 10966.
(10) Longenberger, L.; Mills, G. *J. Phys. Chem.* **1995**, *99*, 475.
(11) Gregg, S. J.; Sing, K. S. W. *Adsorption, Surface Area and Porosity*; Acamedic: London, 1982.

JA054023V